Computational and Structural Biotechnology Journal 23 (2024) 3527–3536

Contents lists available at ScienceDirect

Computational and Structural Biotechnology Journal

journal homepage: www.elsevier.com/locate/csbj

Subgenomic flaviviral RNAs and human proteins: *in silico* exploration of anti-host defense mechanisms

Riccardo Delli Ponti *, Andrea Vandelli, Gian Gaetano Tartaglia *

Centre for Human Technologies, Istituto Italiano di Tecnologia, Via Enrico Melen, 83, Genova GE 16152, Italy

ARTICLE INFO

Keywords:
Protein RNA interaction
RNA viruses
Flaviviruses
RNA secondary structure
Viral host-defense evasion

ABSTRACT

Flaviviruses pose significant global health threats, infecting over 300 million people annually. Among their evasion strategies, the production of subgenomic flaviviral RNAs (sfRNAs) from the 3′ UTR of viral genomes is particularly notable. Utilizing a comprehensive *in silico* approach with the *cat*RAPID algorithm, we analyzed over 300,000 interactions between sfRNAs and human proteins derived from more than 8000 flavivirus genomes, including Dengue, Zika, Yellow Fever, West Nile, and Japanese Encephalitis viruses. By providing the first extensive atlas of sfRNA interactions, we offer new insights into how flaviviruses can manipulate host cellular machinery to facilitate viral survival and persistence. Our study not only validated known interactions but also revealed novel human proteins that could be involved in sfRNA-mediated host defense evasion, including helicases, splicing factors, and chemokines. These findings significantly expand the known interactome of sfRNAs with human proteins, underscoring their role in modulating host cellular pathways. Intriguingly, we predict interaction with stress granules, a critical component of the cellular response to viral infection, suggesting a mechanism by which flaviviruses inhibit their formation to evade host defenses. Moreover, a set of highly-interacting proteins in common among the sfRNAs showed predictive power to identify sfRNA-forming regions, highlighting how protein signatures could be used to annotate viruses. This atlas not only serves as a resource for exploring therapeutic targets but also aids in the identification of sfRNA biomarkers for improved flavivirus diagnostics.

1. Introduction

Flaviviruses are a class of single-stranded RNA viruses, with their genome comprising one open-reading frame, encoding for 10 genes flanked by 5′ and 3′ UTR [1,2]. Several flaviviruses are arboviruses having mosquitoes as intermediary hosts, including Dengue virus (DENV), Zika virus (ZIKV), Yellow Fever virus (YFV), West Nile virus (WNV) and Japanese Encephalitis virus (JEV). While flaviviruses are more highly predominant in tropical environments, global warming is moving the threat toward Europe and North America due to the changing habitat of the hosting mosquito. DENV has already been detected as endemic in different European countries, while West Nile virus (WNV) has been endemic in the USA since 1999 [3]. According to recent estimates, > 300 million people are in danger of potentially contracting Dengue virus, with > 100 million infections every year [4–6]. RNA viruses have different mechanisms to disrupt the human cellular machinery and innate immune response to guarantee their fitness. Flaviviruses are not an exception, with different mechanisms to avoid the host-defense systems. DENV and hepatitis C virus (HCV) induce rearrangements inside the cellular membrane to compartmentalize their replication machinery and regulate the access of antiviral host proteins [7,8]. Moreover, the majority of flaviviruses, including DENV, HCV, and YFV, can disrupt the interferon (IFN) signaling cascade by cleaving or interacting with the STING protein [9–11]. The viral infection also triggers and alters different cellular mechanisms. RNA splicing was shown to be altered after ZIKV infection, which generates alternative splicing events in > 200 RNAs [12]. Other cellular mechanisms, including RNA editing and decay, are potentially involved in anti-viral response, thus becoming a target to be disrupted by viruses [13–15].

During infection, flaviviruses not only generate copies of their genomic RNA (gRNA) but also smaller RNAs, the subgenomic flaviviral RNAs (sfRNAs). Compared to the gRNAs (~11Kb), sfRNAs are much smaller, around 300–500 nucleotides [16,17]. The sfRNAs are viral fragments generated at the 3′ UTR of the viral genome. The mechanism involves the 5′–3′ exoribonuclease XRN1, a host-specific protein that

* Corresponding authors.
E-mail addresses: riccardo.delliponti@iit.it (R. Delli Ponti), gian.tartaglia@iit.it (G.G. Tartaglia).

https://doi.org/10.1016/j.csbj.2024.09.029
Received 21 June 2024; Received in revised form 29 September 2024; Accepted 29 September 2024
Available online 30 September 2024

binds and progressively digests the viral genome. However, flaviviral genomes possess specific complex and rigid stem-loops (SL) in their 3′ UTR that stall XRN1, especially SL-II, thus preventing further digestion [17–19]. These XRN1-resistant structures are also present in the mosquito vector and tend to be conserved in different flaviviruses [19,20]. The existence of these XRN1-resistant structural elements allows the accumulation of the sfRNAs, partially digested RNA fragments at the 3′ UTR of the flaviviral genomes. The sfRNAs are non-coding RNAs (ncRNAs) and their existence and cellular presence is correlated with the virulence and pathogenicity of each flavivirus [3,16].

The presence of sfRNAs is essential for the pathogenicity of WNV, since mutants lacking sfRNAs were poorly replicating in mice [3,19]. Moreover, the intricated secondary structures at the 3′ UTR are essential for the formation and functionality of sfRNAs [19]. Due to their high-concentration and complex secondary structures, it is speculated that sfRNAs can act as protein sponges with an anti host-defence function. Different studies focused on characterizing the human proteins binding to the sfRNA or the 3′ UTR, especially of DENV and ZIKV [21,22]. The cellular functions disrupted by the binding of human proteins with sfRNAs include RNAi and innate immunity, and more specifically the interferon response. However, experimental works mainly focused on DENV and ZIKV. Most studies typically rely on a single representative genome for each virus and only few high-binding protein candidates are consistently identified across different studies.

In this work, we used > 8000 flaviviral genomes coming from DENV, ZIKV, WNV, JEV and YFV to generate > 300,000 in-silico interactions between sfRNAs and human proteins. We selected only arboviruses due to the primary concern related to global warming and their rapid spread. Among arboviruses, we chose the most medically relevant ones, particularly those identified as major concerns by the CDC (www.cdc.gov/vhf/virus-families/flaviviridae.html) [6,23]. Our objective is to study the ability of sfRNAs to interfere with the human RBP network. We were able to identify several mechanisms altered by the binding of human proteins with sfRNAs, categorizing species- and couple-specific proteins between the 5 different flaviviruses. We propose that sfRNAs act as *protein sponges* establishing strong interactions with human RNAs. We identified a core set of 21 proteins in common between the viruses, mainly involving RNA helicases and their interactors. These proteins can be exploited as a proxy to identify sfRNA-forming regions in other flaviviruses, and can be used for further investigations through the *cat*RAPID *omics* algorithm to annotate and further characterize novel viruses.

2. Materials and Methods

2.1. Sequence and structural studies

We used *CD-HIT* [24] to reduce the sequence redundancy at 90 % for all the sfRNAs in our set. We then used *Emboss needleall* [25] to compute the pairwise sequence identity. The *CROSS* algorithm [26], with the *Global Score* module, was used to predict secondary structure profiles. The profiles were then employed to extract a secondary structure consensus profile by averaging *CROSS* score for every position.

2.2. sfRNAs dataset creations

We downloaded the complete genomes of five different flaviviruses: Dengue virus (DENV), Zika virus (ZIKV), West Nile virus (WNV), Japanese Encephalitis virus (JEV), and Yellow Fever virus (YFV). The DENV and ZIKV genomes were sourced from the Virus Pathogen Resource (VIPR), now known as the Bacterial and Viral Bioinformatics Resource Center (Bv-Brc), and comprised over 5000 and 1000 genomes respectively. The genomes for WNV, JEV, and YFV were obtained from the National Center for Biotechnology Information (NCBI), as detailed in Table 1. After downloading the complete genomes, we filtered out genomes with unknown nucleotides (any number of "N" in their genomes).

Table 1
Information about the dataset used in our analysis, from the original downloaded genomes to the sfRNAs obtained by reducing the sequence redundancy.

Virus	Original genomes	Complete Genomes	Redundancy 90 %
DENV	5330	3893	129
ZIKV	1029	904	15
WNV	1850	1660	49
JEV	434	317	15
YFV	434	198	18

After that, we selected the last 500 nt at the 3′ UTRs of all the > 8000 genomes as representatives of the sfRNAs, accordingly to the coordinates of the XRN1-stalling region in DENV and WNV ([16]; Supplementary Figure 1). These 500 nt fragments were then filtered for sequence similarity using CD-HIT (90 % redundancy; [24]).

2.3. Predicting protein-RNA interactions

Interactions between the viral sfRNAs sequences and the human RNA-binding proteome (RBPome) were predicted using *cat*RAPID *omics* [27], an algorithm to estimate the binding propensity of protein–RNA pairs by combining secondary structure, hydrogen bonding and van der Waals contributions. The predictions of the viral sequences against ~1500 human RNA-binding proteins (RBPs) are available at the following links:

ZIKV.
http://crg-webservice.s3.amazonaws.com/submissions/2021–04/351700/output/index.html?unlock=c3e033d661.

JEV.
http://crg-webservice.s3.amazonaws.com/submissions/2021–04/352201/output/index.html?unlock=cdaa7858e1.

YFV.
http://crg-webservice.s3.amazonaws.com/submissions/2021–04/352204/output/index.html?unlock=b61079c43e.

DENV.
http://crg-webservice.s3.amazonaws.com/submissions/2021–04/351702/output/index.html?unlock= 57c29a2684.

WNV.
http://crg-webservice.s3.amazonaws.com/submissions/2021–04/351706/output/index.html?unlock= 4d5a11192f.

The output is filtered according to the *Z*-score, which is the interaction propensity normalized by the mean and standard deviation calculated over the reference RBP set (http://s.tartaglialab.com/static_files/shared/faqs.html#4). We then selected a threshold of Z-score > 1.5 to assess the most relevant interactions, a method employed in previous publications [28]. Consequently, proteins with at least one interaction with a Z-score > 1.5 for a specific sfRNA were considered highly interacting with that virus. Proteins having Z-score > 1.5 only for a selected virus, or the interaction of two viruses, were considered as species- or couple-specific.

2.4. Selecting and comparing experimental proteins

To validate the quality of our predictions, we used a set of known experimental-validated proteins interacting with DENV sfRNA and 3′ UTR [21,22]. For sfRNA-specific proteins, from the original paper, we selected only the proteins specific for DENV (21 proteins). Regarding the 3′-specific proteins, we selected only the proteins with an enrichment > 1.5 (experimental vs control ratio) in any replicate for any DENV serotype, as suggested by the authors of the manuscript (27 proteins). When comparing the interactions between the sfRNAs and the human RBPome, we integrated experimentally validated proteins not present in the original RBPome as custom libraries inside *cat*RAPID *omics* [27]. To check how well these proteins are predicted, we ranked the Z-score of all the predicted interactions (>300,000 interactions between sfRNAs and

human proteins). Then, we selected the top-ranking 10 interactions for each experimentally validated protein, and we checked how well they performed in the top ranked percentage of the overall distribution (Fig. 1).

2.5. GO enrichment analysis

We used GOrilla for the main GO enrichment analysis, using the entire human proteome as background [29]. The P-values of the selected GOs were used as the main input to draw figures.

2.6. eCLIP analysis and the BPI index

RNA interactions for 151 RBPs were retrieved from eCLIP experiments performed in K562 and HepG2 cell lines. In order to measure the fraction of protein binders for each transcript, we applied stringent cut-offs [$-\log_{10}(p\text{-value}) > 5$ and log2(fold_enrichment) > 3] as suggested in the original paper [30]. The coordinates of the peaks were mapped to human transcripts using the GRCh38 reference genome. From these interactions, we retrieved the list of the 100 most contacted transcripts.

We implemented a Binding Promiscuity Index (BPI) to understand if a RNA molecule has a really high-number of interactions in our dataset. The BPI is calculated as the number of strong interactions (Z-score>1.5) in our dataset normalised by the number of transcripts present in each viral species:

$$\frac{n(z > 1.5)}{number\ of\ sequences}$$

where z is the Z-score and n is the number of times this score is > 1.5. We did not normalize for the sequence length since every sequence in our dataset is of 500 nucleotides. As control, we selected the last 500 nt at the 3′ UTR of the most interacting 100 mRNAs, plus lncRNAs and mRNAs downloaded from BioMart (Ensembl version 111) of exactly 500 nt in length.

2.7. Searching for experimental-based RBP motives

We collected conserved RNA binding motives coming from different experimental techniques (eCLIP, Bind-n-Seq, PDB, etc.) [31]. These 5-nucleotide long motives were obtained from human RBPs or, when not available, orthologous RBPs with which they share at least 70 % sequence identity. Each motif is represented by a position-specific probability matrix in MEME format, for a total of 73 motives.

We used *Fimo* web server [32] to search for the previously collected motives inside our sfRNAs. *Fimo* assigned to each motive a P-value and a score. The higher the score, the higher the confidence of a motif to be inside the sequence. In our analysis, we used increasing P-value thresholds to define high-confidence motives ($P < 0.001$ and $P < 0.01$) and then ranked the resulting occurrences by the *Fimo* score. Depending on the threshold applied, we were able to identify a different number of highly interacting DENV proteins (5 and 14 respectively; on a total of 15 proteins with a known experimental motif).

2.8. Granule forming predictions

We used the 97 WNV-specific protein sequences as input for *cat*-GRANULE, an algorithm to predict the granule-forming propensity of selected proteins [33]. Proteins with a score > 0 have a propensity to be involved in granule formation. To study the significance of these findings, we then selected from the RBPome 97 random proteins, and checked how many of them have a score > 0. We did this random sampling for 10,000 times and used that information to build the p-value

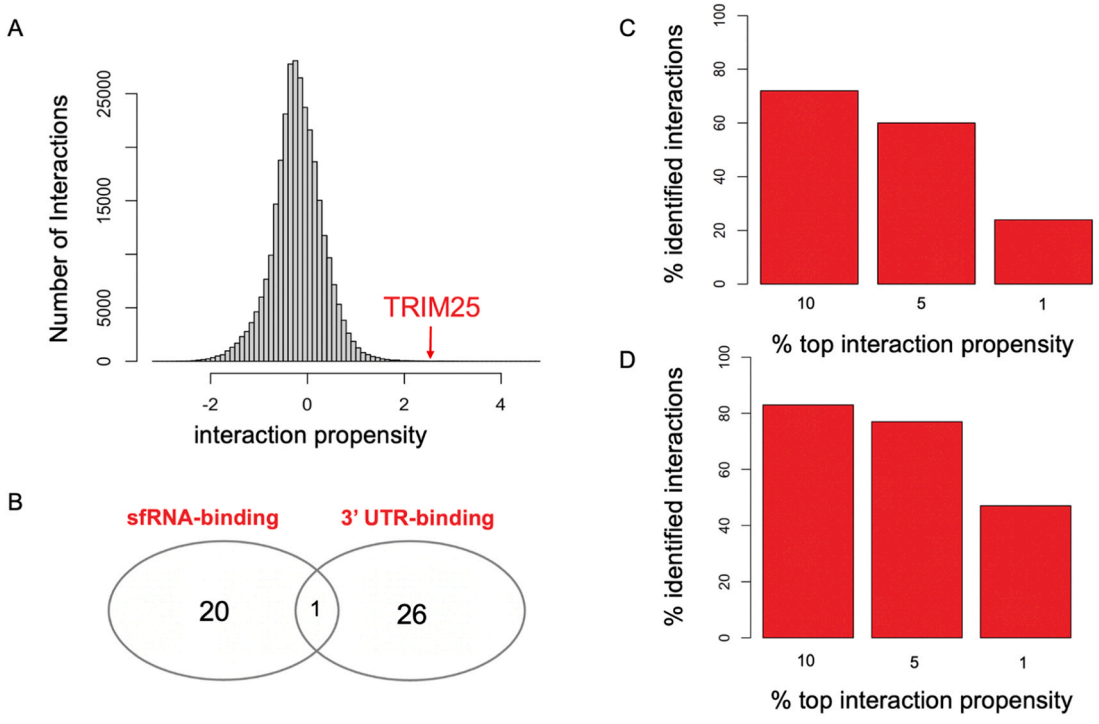

Fig. 1. **(A)** Histogram showing the interaction propensity (catRAPID Z-score) between the human proteome and DENV sfRNAs. Interactions with a Z-score > 1.5 are considered high interactions. TRIM25, known interactor of DENV sfRNAs, is identified with a Z-score $= 2.33$. **(B)** Proteins used as testing for our approach, experimentally validated to interact with DENV sfRNA (*Michalski et al.*) [21] and 3′ UTR (*Liao et al.*) [22]). Barplot showing how the experimentally validated proteins interacting with **(C)** DENV sfRNA and (**D**) DENV 3′ UTR are predicted by catRAPID. For each protein, we selected the best 10 interactions (Z-score) against all DENV sfRNAs. We then checked how these interactions fall inside the distribution of the human proteome interacting with DENV fragments. The proteins are well-predicted, with ~70 % of the interactions falling in the top 10 % of all the ranked interactions between DENV sfRNAs and the human proteome and with ~80 % of the interactions falling in the top 5 % of all the ranked interactions regarding DENV sfRNAs.

for the 97 WNV-specific proteins.

2.9. Checking the predictive power of custom protein libraries

We employed *cat*RAPID *library* [27] to build a custom library comprising only the 21 proteins highly interacting with all the flaviviruses. This library was fed to *cat*RAPID *omics* to predict the individual interactome. We then used this library (ID: 792654) to identify potential sfRNA-forming regions in other flaviviruses. To do that, we divided the Murray Valley virus genome in non-overlapping regions of 500 nucleotides (KF751870; NCBI). Then, we checked how many of the 21 proteins have a Z-score > 1.5 for every region. The higher the proteins with a Z-score > 1.5, the higher the possibility of that viral region to be involved in sfRNA formation. Interested users can run the library at the following site by using the ID 792654 under custom dataset: http://service.tartaglialab.com/update_submission/806477/40da01a38d.

3. Results

3.1. Selection of representative sfRNAs for five flaviviruses

To understand the mechanisms associated with flavivirus infection, we computed a large set of interactions between sfRNAs and human RNA-binding proteins (RBPs). We first downloaded > 8000 genomes of the best known flaviviruses (DENV, ZIKV, WNV, JEV, YFV) available from different sources (Table 1). To select viral fragments at the 3′ UTR encoding for the sfRNAs, we used information coming from the stalling region of XRN1. We note that the complex secondary structure of ~70 nucleotides responsible for blocking XRN1 cannot be converted into motives (scannable on new sequences) by *RNAinverse* due to its complexity [34]. For this reason, we used the known coordinates of XRN1-stalling structure according to DENV and WNV literature [16], and used them to select the fragments at the 3′ UTR of multiple DENV and WNV genomes (Supplementary Figure 1). While for DENV the fragments have a length of roughly 400 nt, in the case of WNV we observed a prevalence of ~500 nt fragments. Knowing that sfRNAs tend to be between 300–500 nt [16,17], and to facilitate comparisons during the computational analysis, we used fragments of 500 nt at the 3′ UTR as representatives for sfRNAs. After selecting the 500 nt fragments, we reduced the intra-species redundancy with *CD-HIT* (90 %, [24]), and used the retrieved fragments as representative sfRNAs for the following analysis on DENV, ZIKV, JEV, WNV, YFV.

3.2. General characteristics of the sfRNAs

After removing sequence redundancy from our dataset, the average pairwise sequence identity among all flavivirus genomes is approximately 40 % (see Supplementary Figure 2**A**). These findings imply that the shared mechanisms of sfRNAs across different viruses are not solely determined by their sequence similarity, particularly after selecting representative fragments with reduced sequence identity. Notably, the 3′ UTR region, which encodes for sfRNA formation, has been shown to be stable in DENV, both through predictions and experimental validations [35]. Moreover, we find the sfRNA fragments to be highly structured based on the predicted secondary structure consensus profile, as expected from literature (Supplementary Figure 2B, [16,26]). Since the secondary structure is a key element for the stalling of XRN1, complex secondary structures are directly linked to the sfRNAs activity.

3.3. TRIM25 and other known proteins binding sfRNAs

We utilized the *cat*RAPID *omics* [27] algorithm to construct an *in silico* interactome of sfRNAs derived from more than 8000 flavivirus genomes. This analysis generated approximately 350,000 interactions with human RNA-binding proteins (RBPs), with around 200,000 interactions specifically associated with the Dengue virus (DENV) (Fig. 1**A**). Strong protein-RNA interactions are characterized by a Z-score > 1.5, in agreement with previous studies [28,36]. To verify the accuracy of our predictions, we analyzed known human interactors of DENV sfRNAs. An example of such a protein is TRIM25, which is known to bind to DENV sfRNA [37]. This binding inhibits the interferon expression, thus promoting DENV fitness. In our analysis, TRIM25 is predicted as a high-level interactor of DENV sfRNA, with a Z-score of 2.33, falling in the top 5 % of all the ranked interactions between DENV sfRNAs and human proteins (Fig. 1**A**).

To further validate our predictions, we used a set of experimental-validated proteins from previous studies, including proteins interacting with the sfRNA and the 3′ UTR of DENV [21,22]. We selected the proteins specifically interacting with DENV sfRNA (21 proteins; [21]) and the high-specific proteins interacting with the DENV 3′ UTR (27 proteins; **Material and Methods:** Selecting and comparing experimental proteins; [22]). We note that the two sets of highly-specific proteins have only one protein in common (Fig. 1**B**). After ranking all the predicted DENV interactions, we checked for each experimentally-validated protein how the best 10 interactions against DENV sfRNAs fall inside the complete distribution of human proteins interacting with DENV fragments (Fig. 1**C, D**). The experimentally validated proteins interacting with DENV sfRNA are very well identified by our method, with 70 % of the interactions falling in the top 10 % ranked interactions and 60 % of them are also in the top 5 % (Fig. 1**C**). The predictions are even more significant for the experimentally validated proteins interacting with DENV 3′ UTR, with 80 % of the predicted interactions falling in the top 5 %, and around 50 % of them also falling in the top 1 % of all the interactions between DENV fragments and the entire human proteome (Fig. 1**D**). We further expanded our analysis by comparing our highly-interacting DENV proteins (Z-score > 1.5) with known binding motives collected from different experimental techniques (eCLIP, Bind-n-Seq, etc…; Supplementary Figure 3; [31]). Interestingly, we identified 15 proteins from our set with an experimentally validated motif (5 nt motives; Supplementary Figure 3**A**). When analyzing the presence of motifs in our set of sfRNAs, 5 out of 15 proteins have a motif identified on the sfRNAs (p-value < 0.001; Supplementary Figure 3B), and 14 out of 15 with a less stringent p-value (p < 0.01). Interestingly, if we rank the motive-identified proteins by *Fimo* score (tool employed to identify sequence-based motives, [32]), the first protein identified is DHX58, a helicase mediating the antiviral signaling [38].

These results highlight the power of our predictions: we are not only able to correctly identify the binding of TRIM25 with DENV sfRNA, but our results also correctly classify two slightly-overlapping sets of experimental-validated proteins coming from two different studies. Moreover, we were able to provide a huge amount of novel high-confidence interactions, highlighting the potential of our analysis to further characterize sfRNAs.

3.4. Expanding the sfRNA interactome with human proteins

To further expand the list of human proteins interacting with sfRNAs, and to consolidate the role of sfRNAs as anti host-defense mechanism, we studied the complete *in silico* interactome of the sfRNAs of DENV, ZIKV, JEV, YFV, and WNV. In this analysis, we focused on proteins with a high interaction propensity, selecting only those with a Z-score greater than 1.5 (Supplementary Table 1). This selective approach allowed us to pinpoint proteins that are specific to each virus species, as well as core proteins that are common across multiple flaviviruses, thereby providing insights into both unique and shared interaction patterns (Fig. 2**A**). DENV has > 200 highly-interacting proteins, with 47 proteins that are specific only to DENV. This is in contrast with ZIKV, which only has 34 highly interacting proteins and zero specific proteins. We used ZIKV as a reference to assess the significance of our findings. When using ZIKV fragments of ~412 nt, which is closer to the actual sfRNA length, we obtained 25 highly interacting proteins. The set of 34 identified using

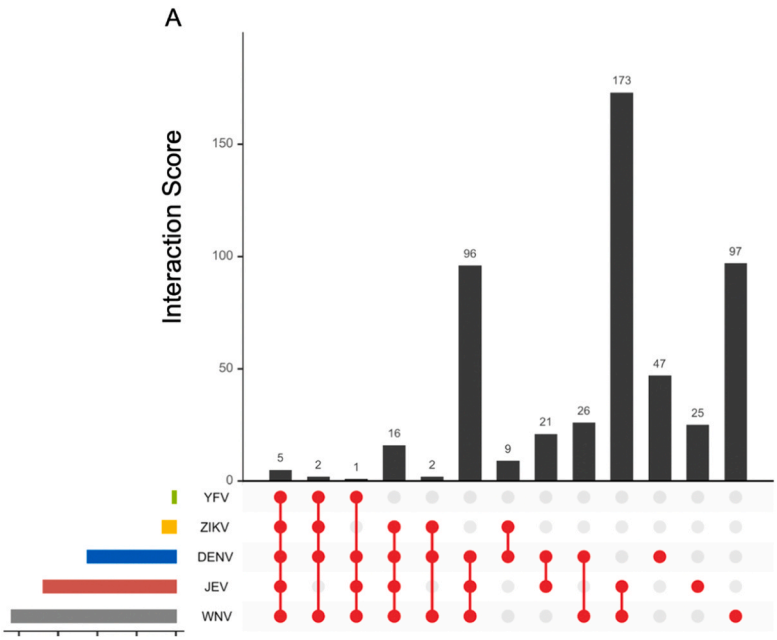

B

Protein	Description	Length
DDX1	ATP-dependent RNA helicase	740
NKRF	NF-kappa-B-repressing factor	690
CSTF3	Cleavage stimulation factor subunit 3	717
TRM1L	TRMT1-like protein	733
NUFP2	Nuclear FMR1-interacting protein 2	695

Fig. 2. **(A)** Upset plot showing the highly interacting proteins (Z-score > 1.5) in common between the 5 different flaviviruses. The bottom-left barplot shows the total high-interacting proteins for each virus. The red dots highlight the intersection reported in the upper barplot. Five proteins are highly interacting with all the sfRNAs. **(B)** Table highlighting the characteristics of the five proteins in common between the five different flaviviruses.

500-nt fragments includes the 25 from the 412-nt fragments, and when compared to the background of ~1500 proteins, the two sets are very significantly overlapping, with a p-value $< 3.9 \times 10^{-47}$, supporting the robustness of our results. WNV shows the highest number of highly-interacting proteins (>400), with 97 proteins specific only to WNV. By checking proteins highly interacting with sfRNAs of all the flaviviruses, we identified five proteins (DDX1, NKRF, CSTF3, TRM1L, NUFP2; Fig. 2**B**). Among these five proteins, we found DDX1, an important helicase involved in host-defense mechanisms during viral infections [39]. NKRF is a regulator of DHX15, another RNA helicase involved in RNA processing and antiviral innate immunity [40], which was also seen to be inhibited by miR-301a during JEV infection [41]. Another example is NUFP2, a FMR1-interacting protein directly antagonized by the sfRNA of ZIKV [42].

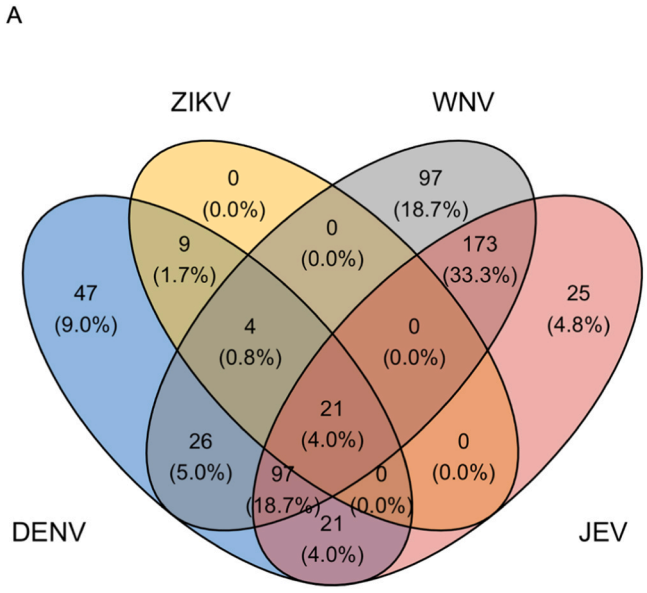

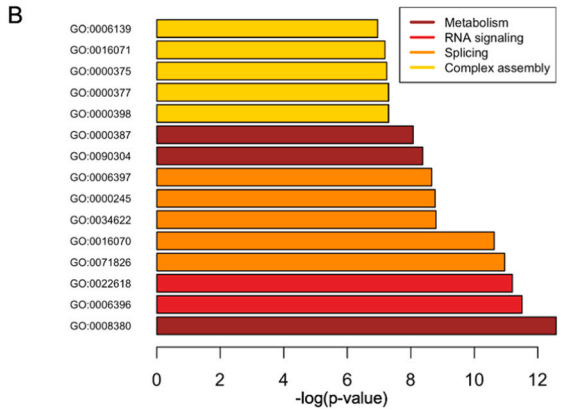

C

GO	Description	P-value
GO:0008380	RNA splicing	3.45E-6
GO:0006396	RNA processing	1.01E-5
GO:0022618	Ribonucleoprotein complex assembly	1.37E-5
GO:0016070	RNA metabolic process	2.42E-5
GO:0034622	Cellular protein-containing complex assembly	1.52E-4
GO:0000245	Spliceosomal complex assembly	1.56E-4
GO:0006397	mRNA processing	1.74E-4

Fig. 3. **(A)** Venn diagram showing the high-interacting proteins (Z-score > 1.5) in common among the 4 different flaviviruses. 21 proteins are considered highly interactive with all the viruses. The percentage represents the reported fraction against the total amount of proteins. **(B)** Barplot showing the p-value of the most significant GOs identified from the enrichment of the 21 common proteins. Terms associated with similar mechanisms share the same colours. **(C)** Table extracted from GOrilla showing specific significant GO terms from the enrichment of the 21 common proteins.

To further validate the specificity of these proteins for the 3′ region of flaviviruses, we checked the interactions between these 5 proteins and the 3′ region (500 nt) of HIV-1 (GenBank: AF033819.3). None of the sfRNA-specific proteins show a Z-score > 1.5 in HIV. The fact that these five proteins are found highly interacting with the sfRNAs of all the flaviviruses may indicate that the presence of sfRNAs could be a common mechanism employed by these viruses to bypass the host immune defenses, either by directly binding to important factors such as RNA helicases or by hijacking regulators of those proteins.

To expand our selection of core sfRNA-interacting proteins, since YFV has only eight highly interacting proteins, we decided to restrict the analysis by selecting the proteins in common between the other four flaviviruses. For this reason, we focused on the 21 proteins highly interacting with DENV, ZIKV, JEV, WNV (Fig. 3**A;** Supplementary Table 2). Also in this case, none of the 21 proteins was found highly-interacting in HIV-1, highlighting the specificity of these proteins. By looking at the biological processes in which these proteins are involved, we found a significant enrichment for RNA splicing, processing, metabolism, and ribonucleoprotein complex assembly (Fig. 3**B, C**). This enrichment already highlights the importance of sfRNAs for anti host-defense mechanisms, considering how altering these cellular host processes could disrupt the cellular machinery, promoting viral fitness. RNA splicing was already identified as the mechanism comprising the largest group of human interacting proteins, hence appearing as a highly disrupted mechanism by the presence of sfRNAs [21]. Overall, we found evidence in literature related to flaviviruses and potential anti host-defense functions for the majority of the proteins in this set. For example, HMGN2, CSTF, and RMB39 are differently regulated upon flavivirus infection, especially in DENV [21,43,44]. We also identified several proteins involved in splicing, including LSM2 and CCNL2. Surprisingly, in this set we also find SRP54 and SRP9, pro-viral proteins and negative regulators of the IFN response [45]. Further experiments are needed to elucidate the extent of these proteins' binding to the sfRNAs, since their presence is supporting viral fitness.

The protein L10K, produced by the gene C19orf53, is an interferon-stimulated gene (ISG) product still not well characterized. However, C19orf53 is found in IFN cDNA libraries together with C19orf66, a recently characterized ISG involved in the antiviral response against DENV and JEV [46,47]. Because of these similarities, L10K is a very promising candidate for further studies to better understand the sfRNAs contribution and the interferon response of the flaviviruses.

3.5. Couple- and species-specific proteins and disrupted mechanisms

JEV and WNV (JEV-WNV) share the highest number of common high-interacting proteins (173 proteins), while DENV-JEV and DENV-WNV have a similar number of common high-interactive proteins (21 and 26 respectively; Fig. 4). As in the previous analysis, we were able to identify known disrupted mechanisms, including proteins associated with RNA processing and RNA metabolism (Supplementary Figure 4). With the exception of the couple DENV-WNV (Fig. 4**A**), by looking at the molecular function of the couple-specific proteins, we found more specific processes. For example, the G protein-coupled receptor signaling pathway is identified as enriched in the proteins specific to WNV-JEV (Fig. 4**B**), a mechanism known to be hijacked during viral infection and tumorigenesis [48]. Moreover, proteins involved in chemokines activity and signaling are also highly binding WNV-JEV sfRNA, a very interesting result since chemokines are crucial for the control of viral infections and part of the IFN cascade [49]. RNA helicases are highly binding the sfRNAs of DENV-JEV, a class of proteins known for their antiviral activity, already reported as a disrupted mechanism for the core 21 proteins (Fig. 4**C**). Moreover, these sfRNAs seem to compete with proteins binding the 3′ UTR of host mRNAs, thus disrupting the post-transcriptional regulation.

We also focused on species-specific proteins, those that bind with high affinity exclusively to a particular virus. As previously reported in our study (see section: **Expanding the sfRNA interactome with human proteins**), WNV shows the highest number of species-specific

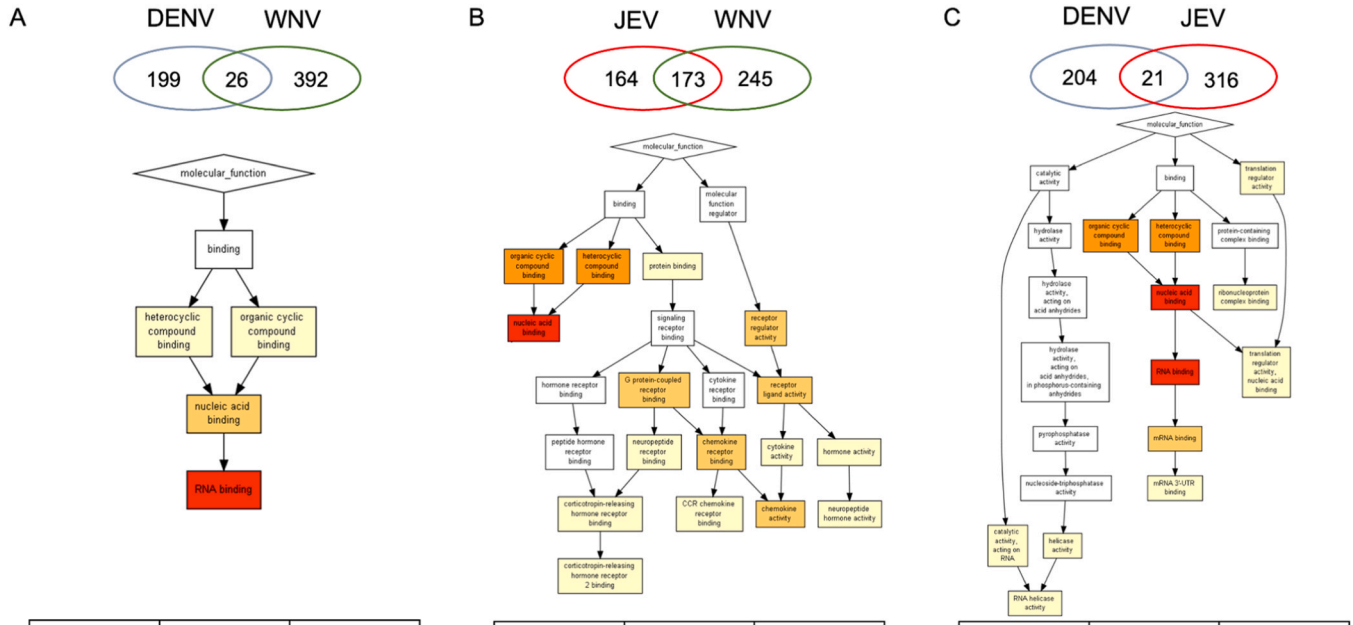

GO:0003723	RNA binding	2.41E-11
GO:1901673	heterocyclic compound binding	2.02E-5

GO:0001664	G protein-coupled receptor binding	2.13E-7
GO:0008009	chemokine activity	1.66E-6
GO:0042379	chemokine receptor binding	6.01E-6

GO:0003724	RNA helicase activity	4.23E-5
GO:0003730	mRNA 3'-UTR binding	6.56E-5
GO:0043021	ribonucleoprotein complex binding	2.23E-4

Fig. 4. **(A)** Enrichment analysis of the 26 proteins highly interacting specifically with DENV and WNV. **(B)** Enrichment analysis of the 173 proteins highly interacting specifically with JEV and WNV. **(C)** Enrichment analysis of the 21 proteins highly interacting specifically with DENV and JEV. In each panel, the GO pathway and summary table were extracted from GOrilla.

proteins (Supplementary Figure 5). These proteins are involved in RNA metabolism and RNA processing, but are also implicated in more specific functions, for example as structural constituents of ribosomes, especially when comparing with more generic functions as the JEV-specific proteins (Supplementary Figure 6). Interestingly, DENV-specific proteins are involved in the binding with the poly-U, poly-A, and 3′ UTR of the mRNAs (Supplementary Figure 7), highlighting again the possible competition with host mRNAs for the binding. Moreover, viruses have different mechanisms to disrupt the poly-A binding in order to inhibit host-translation, for example by cleaving or displacing proteins [50]. In this case, we speculate that DENV could employ a displacing strategy through the sfRNA.

These results coming from couple- and species-specific proteins shed light on potential disrupted mechanisms, including the G protein-coupled signaling, chemokines activity and the heterocyclic compound binding, the latter being particularly relevant considering that some of these molecules have been discovered experimentally to inhibit DENV infection in cell culture [51]. These mechanisms complement the list of processes discovered in the previous analysis of the core-proteins common to all flaviviruses. This shows how crucial mechanisms such as RNA processing and metabolism can be altered during viral infections. Altogether, our results highlight the importance of the sfRNAs to disrupt crucial cellular mechanisms, inhibiting the host-defense system and promoting viral fitness and translation. The results of our enrichment analysis coming from > 8000 flaviviral genomes comprising 5 different viruses are summarized in Table 2.

3.6. Binding promiscuity index and sfRNAs as protein sponges

sfRNAs compromise the host-defense immunity, not only by disrupting important cellular mechanisms but also by directly altering the IFN-mediated immune response and other antiviral-related processes. In the following analysis, we checked whether this hijacking activity could be caused by the sfRNAs acting as *protein sponges*. For this to be the case, sfRNAs should have a high-number of promiscuous but stable interactions. To validate this hypothesis, first, we built a binding promiscuity index (BPI) for each flavivirus as the number of predicted strong interactions (Z-score > 1.5) normalized for the number of sequences in each set. We did not normalize for the RNA length since all the fragments were of 500 nt. While DENV and ZIKV show a low BPI, JEV and especially WNV have a high BPI. Then, we demonstrated the power of the BPI index by showing that JEV and WNV sfRNAs have the potential to bind many host proteins. To achieve this, we employed positive controls based on available experimental data. We analyzed the RNA molecules collected from eCLIP experiments (Fig. 5**A**, **Materials and Methods**; [52]), ranking these RNAs for the number of significant protein contacts. While the majority of the RNAs have very few contacts (Fig. 5**B**), some molecules show a high number of protein interactions.

Table 2
Significant GO terms identified for the common, the species-specific, and couple-specific proteins.

Common GOs	Species-specific GOs		Couple-specific GOs	
GO	**GO**	**Virus**	**GO**	**Virus**
RNA metabolic process	Poly-U RNA binding	DENV	G-coupled receptor signaling pathway	WNV+JEV
RNA processing	mRNA 3′-UTR binding	DENV	Chemokines activity	WNV+JEV
mRNA processing	mRNA export from nucleus	JEV	Chemokines receptor binding	WNV+JEV
RNA splicing	Non-sense mediated decay	WNV	RNA helicase activity	DENV+JEV
Spliceosome complex assembly				
RBP complex assembly	Structural constituent of ribosomes	WNV	Ribonucleoprotein complex binding	DENV+JEV

To test our approach, we selected the 3′ region (500 nt) of the 100 mRNAs with the highest interaction with proteins, according to eCLIP data (Fig. 5**B**), and used these fragments to compute RBP interactions with *cat*RAPID *omics* [27], applying the same procedure of the sfRNAs. Then, we computed the BPI for these RNAs. Moreover, we further validated the BPI by selecting lncRNAs and coding RNAs exactly 500-nt long. While the most interacting RNAs show the highest BPI, as expected, WNV has a higher BPI than lncRNAs and mRNAs of the same length (Fig. 5**C).** These results suggest how sfRNAs, especially WNV, tend to have a high number of protein interactions. Moreover, the sfRNAs compete for the binding with the mRNAs, showing a higher BPI than mRNAs of the same length, highlighting even more their anti host-defense functions.

One of the cellular mechanisms to fight viral infections is the formation of stress granules, which occurs when the viral RNA is sensed by specific proteins such as RIG-I [38], subsequently stalling the rate of mRNAs translation. Unlike solid-like aggregates [53,54], stress granules rapidly assemble to protect the cell during infection and dissolve quickly afterward [28]. In this context, to investigate the anti innate immunity potential of WNV sfRNA, we studied the granule-forming propensity of the > 90 proteins highly-interacting specifically with WNV. This is relevant because, for example, the antiviral mechanism of stress granule formation is inhibited during WNV infection [55,56]. We used *cat*GRANULE [33] to predict the propensity of these proteins to form granules. Interestingly, > 75 % of the WNV-specific proteins exhibit a propensity to undergo phase separation (Supplementary Figure 8). This result is significant when compared to similar random distributions (p-value<0.05; Fig. 5**D; Materials and Methods**: Granule forming predictions). Establishing strong bindings with proteins involved in stress granules or other phase-separated complexes could represent an additional WNV strategy against the host defenses, where the sfRNAs could bind and sequester important components of these organelles to avoid their formation and ensure viral fitness.

3.7. Predicting sfRNA-forming regions employing a subset of human protein interactors

We identified a set of 21 proteins highly-specific and interacting with the sfRNAs of DENV, WNV, JEV, and ZIKV. The specificity of these proteins for the sfRNA-forming regions could be used to further study or characterize novel or less-studied viruses. To test this hypothesis, we used *cat*RAPID *library* [27] to build a custom protein dataset for the 21 proteins to be then used in *cat*RAPID *omics* to predict the interactions. Then, we selected a rare and poorly studied flavivirus, the Murray Valley virus (MVV), which does not come from Asia or South America. MVV is an arbovirus from Australia, forming sfRNAs and exploiting mosquitoes as vectors [2,57]. We studied the complete set of interactions between MVV and the 21 proteins previously identified. For all the fragments of 500 nt, we checked how many of the 21 proteins were highly-interacting (Z-score > 1.5) in every specific region (Fig. 6). Interestingly, the 3′ UTR regions is the only one showing high-interactions with all the 21 proteins, highlighting how this set of proteins can in fact identify sfRNA-forming regions. Moreover, if we perform the same analysis on a non-flavivirus, in this case HIV-1 divided in fragments of 500 nucleotides, we identified only 2/21 highly interacting (Z-score > 1.5) proteins in the region with the highest number of protein-interactions, and not located in the 3′ UTR (Supplementary Figure 9). This result shows how this set of 21 proteins can be used to further study RNA viruses in order to identify regions encoding for sfRNA formation. We propose that this set of proteins could be used to identify other anti host-defense regions in the genome of RNA viruses. For this reason, users can select the custom-library ID (792654) to run specific *cat*RAPID analyses on these proteins (see **Material and Methods**: Running the predictive libraries).

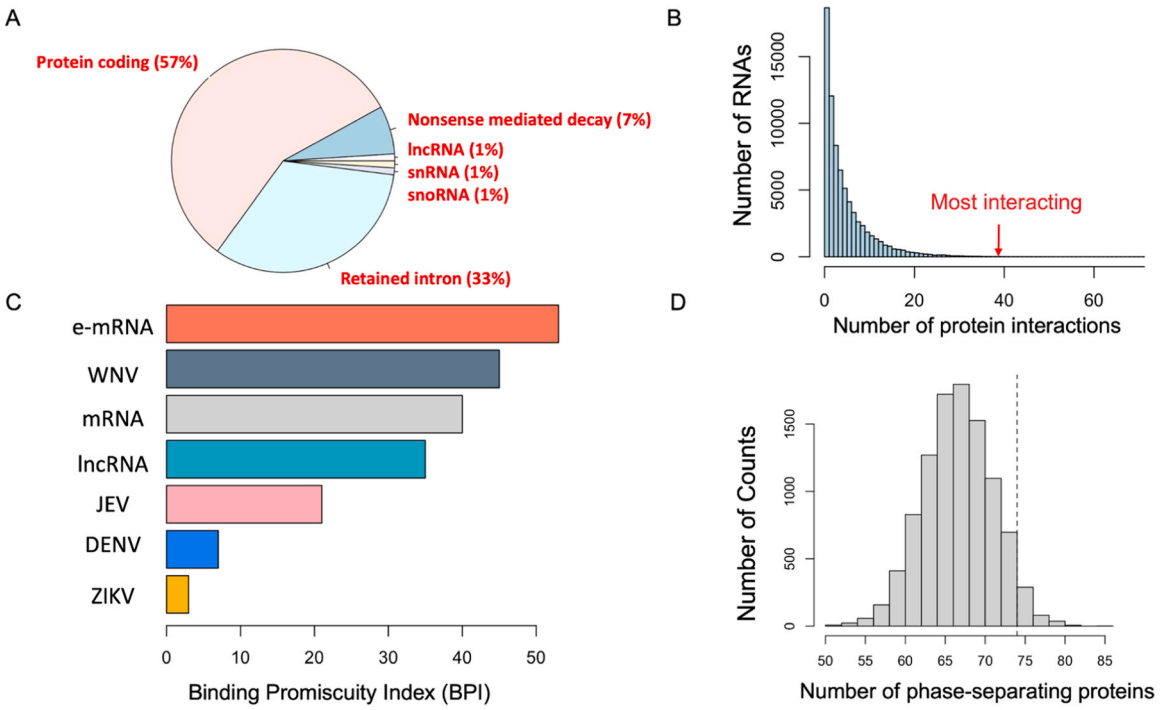

Fig. 5. **(A)** Pie Chart of the eCLIP data, showing the biotype classes of the 100 RNAs most contacted by proteins. **(B)** Histogram of the eCLIP data, showing the number of protein interactions with RNAs. The majority of the RNAs tend to have very few interactions, according to eCLIP data. The average of the 100 most interacting mRNAs is highlighted in the plot. **(C)** Horizontal bar plot showing the Binding Promiscuity Index (BPI) computed for the 5 flaviviruses. The 3′ end of the 100 mRNAs most interacting with proteins (e-mRNAs), according to eCLIP data, plus lncRNAs and mRNAs of 500 nucleotides are used as control. **(D)** *cat*GRANULE significance analysis. For 10,000 times, 97 random proteins were selected from the RBPome, and we checked how many of them have a score > 0, according to *cat*GRANULE. The dashed line represents the threshold of the WNV-specific proteins having a score > 0.

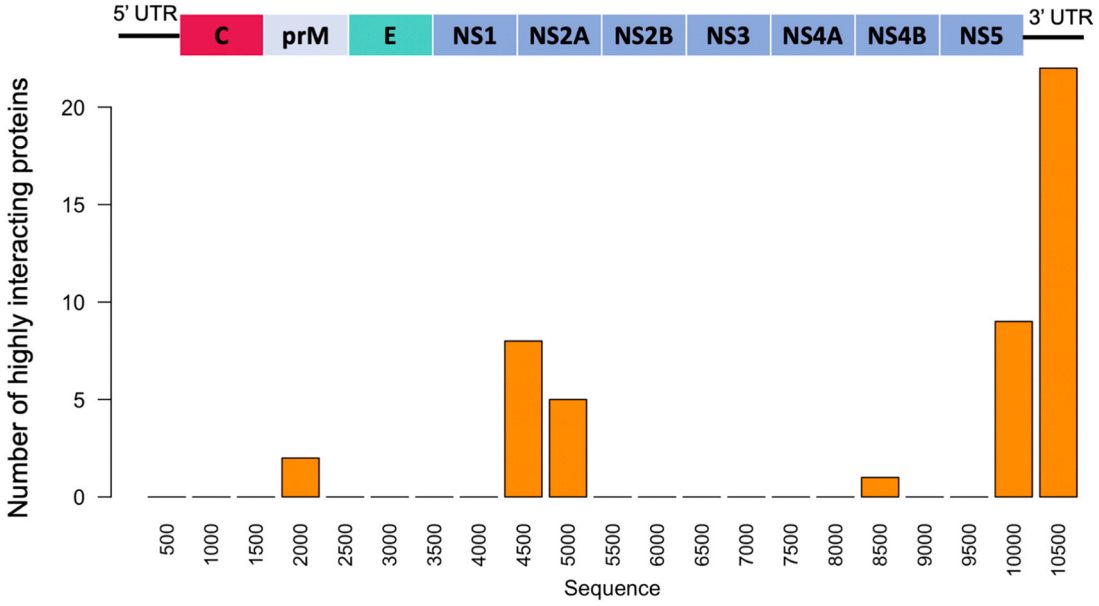

Fig. 6. The genome of the Murray Valley virus (MVV) was divided in fragments of 500 nucleotides. For each region, we highlighted the number of highly interacting proteins (Z-score > 1.5) from the pool of the 21 sfRNA-specific proteins. The 3′ region is the one highly interacting with all the proteins.

4. Discussion

Viruses employ various mechanisms to evade the host's innate immune response, and flaviviruses are no exception, utilizing several strategies to disrupt cellular functions or circumvent the IFN-mediated response. A characteristic mechanism of flaviviruses involves the formation of sfRNAs, which result from the stalling of the XRN1 enzyme at the 3′ UTR of flaviviral genomes. These RNA fragments have been shown to play a crucial role in countering host-defense mechanisms. However, the full extent of sfRNAs' roles was not completely understood due to the limited number of flaviviral genomes analyzed and the few common candidate proteins identified in different studies. For this reason, a computational high-throughput analysis can shed light on new properties and interactions between the human proteome and sfRNAs.

In our research, we analyzed over 8000 genomes from five different flaviviruses (DENV, ZIKV, WNV, JEV, YFV) to examine the predicted in-silico interactome with human proteins. We approximated sfRNAs using 500-nucleotide fragments based on the distribution of fragments generated from XRN1-stalling coordinates. This is a needed approximation due to the lack of high-throughput annotations for the XRN1 stalling coordinates and the complexity of its structure. Our in-silico interactome comprised more than 300,000 interactions between sfRNAs and human proteins. Among the most interacting proteins, we identified known sfRNA interactors, including TRIM25. To further validate our predictions, we utilized two sets of experimentally validated proteins that interact with the DENV sfRNA and its 3′ UTR [21,22].

Supporting the high quality of our predictions, we identified that approximately 70 % of the experimentally validated sfRNA-specific interactions fell within the top 10 % of ranked interactions. Additionally, about 80 % of the predicted interactions involving 3′-specific proteins ranked within the top 5 % of all interactions between DENV fragments and the entire human RNA-binding proteome (RBPome; Fig. 1).

We identified the interactions of each virus, including species-specific proteins: 47 proteins highly interacting specifically only with DENV, 97 with WNV, and 25 with JEV. WNV and JEV showed the highest number of coupled-specific proteins, with 173 proteins interacting only with WNV and JEV. Importantly, 21 proteins were classified as highly interacting with all the flaviviruses, excluding YFV. Among these proteins, we identified different helicases and their interactors, including DDX1, DHX58, and a regulator of DDX15. Knowing the innate antiviral activity of the RNA helicases, it is easy to speculate how the binding with the sfRNAs disrupt this host-defense mechanism, promoting viral fitness. This set of 21 proteins offers a valuable resource for identifying sfRNA-forming regions, as demonstrated by the contrasting results when applied to MVV and HIV. We believe that in the future, interactome-based signatures between viruses and their hosts could be used to annotate novel RNA viruses more comprehensively, with the pool of sfRNA-associated proteins being just one of many potential applications.

We computationally investigated the general mechanisms and functions of human proteins interacting with sfRNAs. The majority of highly interacting proteins are associated with RNA splicing, signaling, and metabolic processes—crucial host cellular functions that are often disrupted by viral infections. Specifically, RNA splicing is the primary mechanism involving most of the proteins bound to DENV sfRNA, as corroborated by experimental data [21]. Species-specific and couple-specific proteins tend to be linked with more targeted anti-host defense mechanisms, such as competing for binding at the 3′ UTR with host coding RNAs or disrupting the activity of RNA helicases and chemokines. These findings shed light on the multiple layers of anti-host defense mechanisms employed by sfRNAs, which can hijack and disrupt general cellular mechanisms common to all flaviviruses, while also displaying alterations specific to each viral species. This is possible due to the numerous strong interactions that sfRNAs can establish with human proteins. We demonstrated that WNV, in particular, has a higher number of strong interactions compared to coding and long non-coding RNAs of the same length. Additionally, WNV appears to be associated with granule-forming proteins, likely to inhibit the formation of stress granules, thereby enhancing viral fitness [28,36]. This supports our hypothesis that sfRNAs not only disrupt and hijack various cellular mechanisms but also function as protein sponges by establishing a high number of potential bindings. We understand how these findings are still speculative, and we hope that future experiments could further validate the results. Our high-throughput *in-silico* approach is the first step in order to further analyze these complex dynamics. Understanding the network of interactions between human proteins and viral genomes can shed new light to the possible host-defense mechanisms of novel viruses.

Future experiments and annotations could only strengthen our work. Having the exact coordinates of the XRN1 stalling region on multiple flaviviral genomes, or even better, a curated dataset of sfRNA sequences, could provide a better resolution than relying on approximated sfRNAs. Moreover, future experiments could further validate the proteins we selected in our computational analysis. We believe that the proteins we identified could be exploited both as a resource and an instrument to further identify and categorise sfRNAs, leading to future experiment-based research toward a more complete understanding of sfRNAs and their interaction with the human cell machinery.

5. Conclusions

In this work, we computed the largest *in silico* interactome of flaviviruses to understand how the accumulation of sfRNAs in human cells can disrupt host-defense mechanisms. Our analysis provided a way to exploit the newly-identified candidate proteins. Indeed, we demonstrated that a set of 21 proteins, which interact with sfRNAs from all the different viruses, can be used as a predictive tool to identify sfRNA-forming regions in other cases, such as the Murray Valley virus—a distinct Australian flavivirus not previously included in our analysis. Researchers can also employ this set of proteins with the *cat*RAPID *library* [27] to characterize novel or understudied flaviviruses. We plan to integrate this information into other algorithms, such as *RNAvigator* [35], to utilize specific protein interactions to identify characteristic features of RNA regions.

Abbreviations

DENV: Dengue virus.
ZIKV: Zika virus.
WNV: West Nile Fever virus.
JEV: Japanese Encephalitis virus.
YFV: Yellow Fever virus.
HCV: Hepatitis C virus.
RBP: RNA binding protein.
UTR: Untranslated region.
GO: Gene ontology.
ss-RNA: Single-stranded RNA.
lncRNA: Long non-coding RNA.
sfRNA: Subgenomic flaviviral RNA.

Funding

The research leading to this work was supported by the ERC ASTRA_855923 (G.G.T.), EIC Pathfinder IVBM4PAP_101098989 (G.G.T.) and PNRR grant from National Centre for Gene Therapy and Drugs based on RNA Technology (CN00000041 EPNRRCN3 (G.G.T.).

CRediT authorship contribution statement

Andrea Vandelli: Writing – review & editing, Writing – original draft, Methodology, Investigation, Formal analysis. **Gian G. Tartaglia:** Writing – review & editing, Writing – original draft, Supervision, Investigation, Funding acquisition. **Riccardo Delli Ponti:** Writing – review & editing, Writing – original draft, Methodology, Investigation, Formal analysis, Conceptualization.

Declaration of Competing Interest

The authors declare that they have no known competing financial interests or personal relationships that could have appeared to influence the work reported in this paper.

Data Availability

The catRAPID interactions are available as individual links in the Material and Methods. The most interacting proteins for all the viruses are available in the Supplementary Table 1**.** The complete list of the 21

proteins interacting with all viruses is available in Supplementary Table 2.

Acknowledgements

The authors would like to thank the other members of Tartaglia's group and Roland Huber for the useful comments.

Appendix A. Supporting information

Supplementary data associated with this article can be found in the online version at doi:10.1016/j.csbj.2024.09.029.

References

[1] Ramos-Lorente S, Romero-López C, Berzal-Herranz A. Information encoded by the flavivirus genomes beyond the nucleotide sequence. Int J Mol Sci 2021;22.
[2] Chapman EG, Costantino DA, Rabe JL, Moon SL, Wilusz J, Nix JC, et al. The structural basis of pathogenic subgenomic flavivirus RNA (sfRNA) production. Science 2014;344:307–10.
[3] Schuessler A, Funk A, Lazear HM, Cooper DA, Torres S, Daffis S, et al. West Nile virus noncoding subgenomic RNA contributes to viral evasion of the type I interferon-mediated antiviral response. J Virol 2012;86:5708–18.
[4] Bhatt S, Gething PW, Brady OJ, Messina JP, Farlow AW, Moyes CL, et al. The global distribution and burden of dengue. Nature 2013;496:504–7.
[5] Brady OJ, Gething PW, Bhatt S, Messina JP, Brownstein JS, Hoen AG, et al. Refining the global spatial limits of dengue virus transmission by evidence-based consensus. PLoS Negl Trop Dis 2012;6:e1760.
[6] Pierson TC, Diamond MS. The continued threat of emerging flaviviruses. Nat Microbiol 2020;5:796–812.
[7] Scutigliani EM, Kikkert M. Interaction of the innate immune system with positive-strand RNA virus replication organelles. Cytokine Growth Factor Rev 2017;37:17–27.
[8] Ma Z, Damania B. The cGAS-STING defense pathway and its counteraction by viruses. Cell Host Microbe 2016;19:150–8.
[9] Aguirre S, Maestre AM, Pagni S, Patel JR, Savage T, Gutman D, et al. DENV inhibits type I IFN production in infected cells by cleaving human STING. PLoS Pathog 2012;8:e1002934.
[10] Ishikawa H, Ma Z, Barber GN. STING regulates intracellular DNA-mediated, type I interferon-dependent innate immunity. Nature 2009;461:788–92.
[11] Nitta S, Sakamoto N, Nakagawa M, Kakinuma S, Mishima K, Kusano-Kitazume A, et al. Hepatitis C virus NS4B protein targets STING and abrogates RIG-I-mediated type I interferon-dependent innate immunity. Hepatology 2013;57:46–58.
[12] Hu B, Huo Y, Yang L, Chen G, Luo M, Yang J, et al. ZIKV infection effects changes in gene splicing, isoform composition and lncRNA expression in human neural progenitor cells. Virol J 2017;14:217.
[13] Moon SL, Wilusz J. Cytoplasmic viruses: rage against the (cellular RNA decay) machine. PLoS Pathog 2013;9:e1003762.
[14] Chemudupati M, Kenney AD, Bonifati S, Zani A, McMichael TM, Wu L, et al. From APOBEC to ZAP: diverse mechanisms used by cellular restriction factors to inhibit virus infections. Biochim Biophys Acta Mol Cell Res 2019;1866:382–94.
[15] Peng Z-G, Zhao Z-Y, Li Y-P, Wang Y-P, Hao L-H, Fan B, et al. Host apolipoprotein B messenger RNA-editing enzyme catalytic polypeptide-like 3G is an innate defensive factor and drug target against hepatitis C virus. Hepatology 2011;53:1080–9.
[16] Chapman EG, Moon SL, Wilusz J, Kieft JS. RNA structures that resist degradation by Xrn1 produce a pathogenic Dengue virus RNA. eLife 2014;3:e01892.
[17] Slonchak A, Khromykh AA. Subgenomic flaviviral RNAs: what do we know after the first decade of research. Antivir Res 2018;159:13–25.
[18] MacFadden A, O'Donoghue Z, Silva PAGC, Chapman EG, Olsthoorn RC, Sterken MG, et al. Mechanism and structural diversity of exoribonuclease-resistant RNA structures in flaviviral RNAs. Nat Commun 2018;9:119.
[19] Funk A, Truong K, Nagasaki T, Torres S, Floden N, Balmori Melian E, et al. RNA structures required for production of subgenomic flavivirus RNA. J Virol 2010;84:11407–17.
[20] Fiacre L, Pagès N, Albina E, Richardson J, Lecollinet S, Gonzalez G. Molecular determinants of west nile virus virulence and pathogenesis in vertebrate and invertebrate hosts. Int J Mol Sci 2020;21.
[21] Michalski D, Ontiveros JG, Russo J, Charley PA, Anderson JR, Heck AM, et al. Zika virus noncoding sfRNAs sequester multiple host-derived RNA-binding proteins and modulate mRNA decay and splicing during infection. J Biol Chem 2019;294:16282–96.
[22] Liao K-C, Chuo V, Ng WC, Neo SP, Pompon J, Gunaratne J, et al. Identification and characterization of host proteins bound to dengue virus 3′ UTR reveal an antiviral role for quaking proteins. RNA 2018;24:803–14.
[23] Hou B, Chen H, Gao N, An J. Cross-reactive immunity among five medically important mosquito-borne flaviviruses related to human diseases. Viruses 2022;14.
[24] Li W, Godzik A. Cd-hit: a fast program for clustering and comparing large sets of protein or nucleotide sequences. Bioinformatics 2006;22:1658–9.
[25] Rice P, Longden I, Bleasby A. EMBOSS: the european molecular biology open software suite. Trends Genet 2000;16:276–7.
[26] Delli Ponti R, Marti S, Armaos A, Tartaglia GG. A high-throughput approach to profile RNA structure. Nucleic Acids Res 2017;45:e35.
[27] Agostini F, Zanzoni A, Klus P, Marchese D, Cirillo D, Tartaglia GG. catRAPID omics: a web server for large-scale prediction of protein-RNA interactions. Bioinformatics 2013;29:2928–30.
[28] Vandelli A, Monti M, Milanetti E, Armaos A, Rupert J, Zacco E, et al. Structural analysis of SARS-CoV-2 genome and predictions of the human interactome. Nucleic Acids Res 2020;48:11270–83.
[29] Eden E, Navon R, Steinfeld I, Lipson D, Yakhini Z. GOrilla: a tool for discovery and visualization of enriched GO terms in ranked gene lists. BMC Bioinforma 2009;10:48.
[30] Van Nostrand EL, Freese P, Pratt GA, Wang X, Wei X, Xiao R, et al. A large-scale binding and functional map of human RNA-binding proteins. Nature 2020;583:711–9.
[31] Armaos A, Colantoni A, Proietti G, Rupert J, Tartaglia GG. catRAPID omics v2.0: going deeper and wider in the prediction of protein-RNA interactions. Nucleic Acids Res 2021;49:W72–9.
[32] Grant CE, Bailey TL, Noble WS. FIMO: scanning for occurrences of a given motif. Bioinformatics 2011;27:1017–8.
[33] Bolognesi B, Lorenzo Gotor N, Dhar R, Cirillo D, Baldrighi M, Tartaglia GG, et al. A concentration-dependent liquid phase separation can cause toxicity upon increased protein expression. Cell Rep 2016;16:222–31.
[34] Gruber AR, Lorenz R, Bernhart SH, Neuböck R, Hofacker IL. The Vienna RNA websuite. Nucleic Acids Res 2008;36(Web Server issue):W70–4.
[35] Delli Ponti R, Wang J, Wan Y, Huber RG. Rnavigator: a pipeline to identify candidates for functional RNA structure elements. FrontVirol 2022;2.
[36] Vandelli A, Vocino G, Tartaglia GG. Phase separation drives SARS-CoV-2 replication: a hypothesis. Front Mol Biosci 2022;9:893067.
[37] Manokaran G, Finol E, Wang C, Gunaratne J, Bahl J, Ong EZ, et al. Dengue subgenomic RNA binds TRIM25 to inhibit interferon expression for epidemiological fitness. Science 2015;350:217–21.
[38] Rehwinkel J, Gack MU. RIG-I-like receptors: their regulation and roles in RNA sensing. Nat Rev Immunol 2020;20:537–51.
[39] Feng T, Sun T, Li G, Pan W, Wang K, Dai J. DEAD-Box Helicase DDX25 is a negative regulator of type I interferon pathway and facilitates RNA virus infection. Front Cell Infect Microbiol 2017;7:356.
[40] Xing J, Zhou X, Fang M, Zhang E, Minze LJ, Zhang Z. DHX15 is required to control RNA virus-induced intestinal inflammation. Cell Rep 2021;35:109205.
[41] Majumdar A, Basu A. Involvement of host microRNAs in flavivirus-induced neuropathology: an update. J Biosci 2022;47.
[42] Zhang Y, Liang D, Yuan F, Yan Y, Wang Z, Liu P, et al. Replication is the key barrier during the dual-host adaptation of mosquito-borne flaviviruses. Proc Natl Acad Sci USA 2022;119:e2110491119.
[43] Miao M, Yu F, Wang D, Tong Y, Yang L, Xu J, et al. Proteomics profiling of host cell response via protein expression and phosphorylation upon dengue virus infection. Virol Sin 2019;34:549–62.
[44] Bonenfant G, Meng R, Shotwell C, Badu P, Payne AF, Ciota AT, et al. Asian zika virus isolate significantly changes the transcriptional profile and alternative RNA splicing events in a neuroblastoma cell line. Viruses 2020;12.
[45] Barrows NJ, Anglero-Rodriguez Y, Kim B, Jamison SF, Le Sommer C, McGee CE, et al. Dual roles for the ER membrane protein complex in flavivirus infection: viral entry and protein biogenesis. Sci Rep 2019;9:9711.
[46] Yu D, Zhao Y, Pan J, Yang X, Liang Z, Xie S, et al. C19orf66 inhibits Japanese encephalitis virus replication by targeting -1 PRF and the NS3 protein. Virol Sin 2021;36:1443–55.
[47] Suzuki Y, Chin W-X, Han Q, Ichiyama K, Lee CH, Eyo ZW, et al. Characterization of RyDEN (C19orf66) as an interferon-stimulated cellular inhibitor against dengue virus replication. PLoS Pathog 2016;12:e1005357.
[48] Zhang J, Feng H, Xu S, Feng P. Hijacking GPCRs by viral pathogens and tumor. Biochem Pharm 2016;114:69–81.
[49] Melchjorsen J, Sørensen LN, Paludan SR. Expression and function of chemokines during viral infections: from molecular mechanisms to in vivo function. J Leukoc Biol 2003;74:331–43.
[50] Gao J, Tang Y-D, Hu W, Zheng C. When poly(A) binding proteins meet viral infections, including SARS-CoV-2. J Virol 2022;96:e0013622.
[51] García LL, Padilla L, Castaño JC. Inhibitors compounds of the flavivirus replication process. Virol J 2017;14:95.
[52] Van Nostrand EL, Pratt GA, Shishkin AA, Gelboin-Burkhart C, Fang MY, Sundararaman B, et al. Robust transcriptome-wide discovery of RNA-binding protein binding sites with enhanced CLIP (eCLIP). Nat Methods 2016;13:508–14.
[53] Buell AK, Tartaglia GG, Birkett NR, Waudby CA, Vendruscolo M, Salvatella X, et al. Position-dependent electrostatic protection against protein aggregation. Chembiochem 2009;10:1309–12.
[54] Zanzoni A, Marchese D, Agostini F, Bolognesi B, Cirillo D, Botta-Orfila M, et al. Principles of self-organization in biological pathways: a hypothesis on the autogenous association of alpha-synuclein. Nucleic Acids Res 2013;41:9987–98.
[55] Courtney SC, Scherbik SV, Stockman BM, Brinton MA. West nile virus infections suppress early viral RNA synthesis and avoid inducing the cell stress granule response. J Virol 2012;86:3647–57.
[56] Emara MM, Brinton MA. Interaction of TIA-1/TIAR with West Nile and dengue virus products in infected cells interferes with stress granule formation and processing body assembly. Proc Natl Acad Sci USA 2007;104:9041–6.
[57] Bavia L, Mosimann ALP, Aoki MN, Duarte Dos Santos CN. A glance at subgenomic flavivirus RNAs and microRNAs in flavivirus infections. Virol J 2016;13:84.